Available online at www.sciencedirect.com

SciVerse ScienceDirect

Ceramics International 38 (2012) 3197–3201

CERAMICS INTERNATIONAL

www.elsevier.com/locate/ceramint

Fabrication of SnO_2 and SiO_2 nanoparticle-embedded carbon nanofiber composites via co-electrospinning

Geon-Hyoung An, Hyo-Jin Ahn *

Department of Materials Science and Engineering, Seoul National University of Science and Technology, Seoul 139-743, Republic of Korea

Received 22 November 2011; received in revised form 13 December 2011; accepted 13 December 2011
Available online 19 December 2011

Abstract

Carbon nanofiber (CNF) composites composed of SnO_2 and SiO_2 nanoparticles in the CNF were fabricated via a co-electrospinning method, and the weight percentage ratio of the SnO_2 and SiO_2 nanoparticles to the CNF was controlled to investigate their morphology and structural properties. Their structural characteristics and chemical compositions were shown by X-ray diffraction (XRD), X-ray photoelectron spectroscopy (XPS), scanning electron microscopy (SEM), and bright-field transmission electron microscopy (TEM). The TEM energy-dispersive X-ray spectroscopy (EDS) mapping results showed that the SnO_2 and SiO_2 nanoparticles were well distributed in the CNF, implying the successful formation of CNF composites consisting of three types of phases.

Keywords: B. Composites; D. Carbon; Co-electrospinning; Nanofiber; SnO_2 and SiO_2

1. Introduction

Carbon-based materials have recently attracted considerable interest because of their remarkable characteristics, such as their unique structure and physical/chemical properties as well as their application in energy conversion devices, catalysts, and optoelectronics [1,2]. Carbon-based materials exist in various polymorphic forms, namely graphite, carbon nanotubes, graphene, fullerenes, and carbon nanofibers (CNFs), which have peculiar physical and chemical properties. Among these various forms, CNFs, which are typically 50–500 nm in diameter and a few tens of microns in lengths [3], have received a steadily increasing amount of attention in academia and the industry; this is also true for synthesis methods such as chemical vapour deposition (CVD) and electrospinning [4,5]. In particular, electrospinning is one of the most popular methods for fabricating CNFs because of its advantages such as its simplicity, versatility, low-cost, and large-scale productivity [5–7]. Furthermore, CNF composites have recently attracted considerable interest owing to their various applications and peculiar properties. For example, Jung et al. reported the electrochemical properties of Cu_xO-embedded CNFs using an electrospinning method [8]. Ji and Zhang studied MnO_x-loaded porous CNFs for use as anodes in Li-ion batteries, which exhibit large reversible capacity and excellent capacity retention [9]. Nagamine et al. fabricated carbon-core/TiO_2-sheath NFs prepared via electrospinning with an interfacial sol–gel reaction [10]. However, although CNF composites consisting of two types of phases, such as the examples cited above, have been extensively studied, CNF composites consisting of three types of phases have not been studied hitherto. In particular, the introduction of the SnO_2 and SiO_2 nanoparticles embedded into CNF could affect applications relative to energy conversion devices such as Li-ion batteries and electrochemical capacitors as well as the structural and mechanical properties relative to ductility of CNF.

In this study, we have successfully synthesized CNF composites consisting of SnO_2 and SiO_2 nanoparticles. We have also shown their formation and structural characteristics according to the weight percentage ratio of the SnO_2 and SiO_2 nanoparticles to the CNFs by X-ray diffraction (XRD), X-ray photoelectron spectroscopy (XPS), field-emission scanning electron microscopy (FESEM), transmission electron microscopy (TEM), and TEM energy-dispersive X-ray spectroscopy (EDS) mapping.

* Corresponding author. Tel.: +82 2 970 6622; fax: +82 2 973 6657.
E-mail address: hjahn@seoultech.ac.kr (H.-J. Ahn).

0272-8842/$36.00
doi:10.1016/j.ceramint.2011.12.024

2. Experimental

2.1. Experimental

We have synthesized three different types of CNF composites consisting of SnO_2 and SiO_2 nanoparticles in the CNF via co-electrospinning. To synthesize the CNF composites, we set up two coaxial capillaries and then prepared two precursor solutions relative to the core section and the sheath section as shown in Fig. 1. First, in the core section, tetraethylorthosilicate (TEOS, Aldrich) and tin(II) chloride dihydrate ($SnCl_2$, Aldrich) were dissolved in N,N-dimethylformamide (DMF, Aldrich) by stirring the solution for 2 h. Poly(vinylpyrrolidone) (PVP, M_w = 1,300,000 g/mol, Aldrich) was used as a stabilizer to fabricate uniform CNFs and was mixed into the above-dispersed solution for 1 h. To further investigate the morphology and structural properties of the CNF composites, the weight percentage ratios of TEOS and the $SnCl_2$ precursor were controlled at 1:1, 2:2, and 4:4 (referred to be here as samples A, B, and C, respectively). Next, in the sheath section, polyacrylonitrile (PAN, M_w = 150,000 g/mol) and PVP were dissolved in DMF by stirring the solution for 2 h. The two coaxial capillaries were composed of a 26-gauge inner capillary relative to TEOS and the $SnCl_2$ precursors and an 18-gauge outer capillary relative to the PAN precursor. Feeding rates for the core section and the sheath section were fixed at 0.02 ml/h and 0.04 ml/h, respectively. The distance between the tip and the collector was fixed at ~17 cm under a constant voltage of ~17 kV. The humidity was ~30% at room temperature. All the samples were heat-treated at 280 °C for 5 h in air and then carbonized at 800 °C in nitrogen atmosphere (99.999%).

2.2. Characterization

The crystallinity and structural properties of the samples were characterized by the XRD (Rigaku D/Max 2500 V equipped with a Cu K_α source) technique in the range of 10–80°, with a step size of 0.02°. The chemical bonding states and composition of the samples were examined by XPS (ESCALAB 250 equipped with an Al K_α X-ray source) at a base pressure of 2×10^{-9} torr. FESEM (Hitachi S-4700) and TEM (TECNAI F-20) with selected area electron diffraction (SAED) patterns were used to examine the structure and morphology of the samples. To confirm the distributed composition of each phase, TEM-EDS mapping examinations were carried out using a Phillips CM20T/STEM electron microscope equipped with an energy dispersive X-ray spectrometer.

3. Results and discussion

Fig. 2 shows the powder XRD plots for sample A, sample B, sample C, and single CNFs after they are calcined at 800 °C. The single CNFs without SnO_2 and SiO_2 nanoparticles exhibit a broad diffraction peak at 25°, indicating amorphous characteristics. Although samples A and B include SnO_2 and SiO_2 nanoparticles, broad diffraction peaks at 25° are observed owing to a small amount of SnO_2 and SiO_2 at a nano-sized scale. However, in the case of sample C, characteristic diffraction peaks at 26.6°, 33.9°, and 51.8° are observed, corresponding to a SnO_2 phase with tetragonal structure (space group $P4_2/mnm$ [136], JCPDS card No. 77-0447). In addition, no characteristic peaks relative to SiO_2 are observed. The XRD results imply that the CNF composites are composed of crystalline SnO_2 and amorphous SiO_2 embedded in a CNF matrix.

Fig. 3 shows the XPS spectra of the survey data, Si 2*p* core level, and Sn 3*d* core level obtained from samples A, B, and C. In the case of the survey data (Fig. 2(a)), the relative intensities of the Sn spectral peaks at ~486.8 eV and the Si spectral peaks at ~103.2 eV increase with the enhancing weight percentage ratio for the Sn and the Si precursors. This result implies that sample C includes a higher loading of Sn and Si phases embedded in the CNF than samples A and B. The XPS Si 2*p* core-level spectra for the samples (Fig. 3(b)–(d)) are observed at ~103.2 eV, corresponding to elemental Si in SiO_2. The XPS Sn 3*d* core-level spectra for the samples (Fig. 3(e)–(g)) are observed at ~486.8 eV ($3d_{5/2}$) and ~495.2 eV ($3d_{3/2}$),

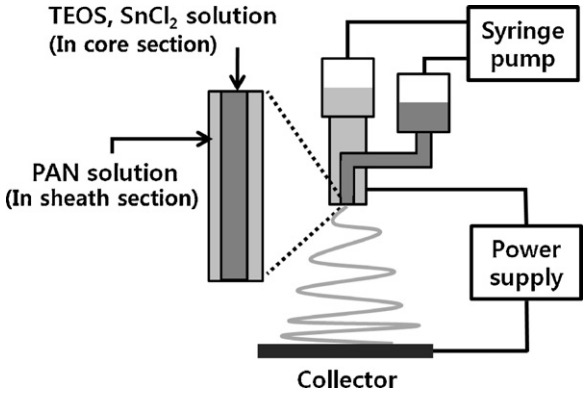

Fig. 1. Enlarged schematic of two coaxial capillaries in co-electrospinning apparatus.

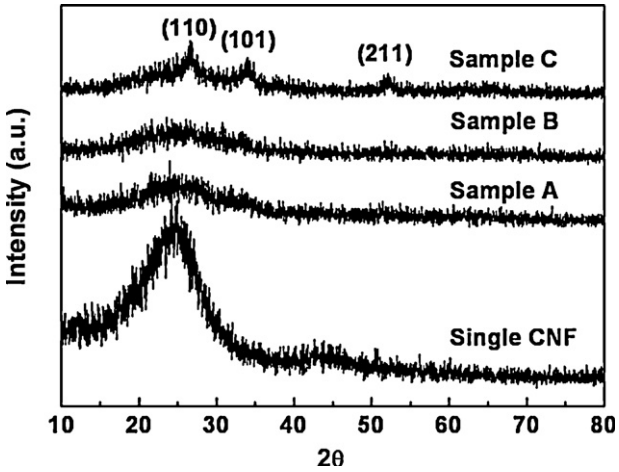

Fig. 2. XRD plots of (a) sample A, (b) sample B, (c) sample C, and single CNF.

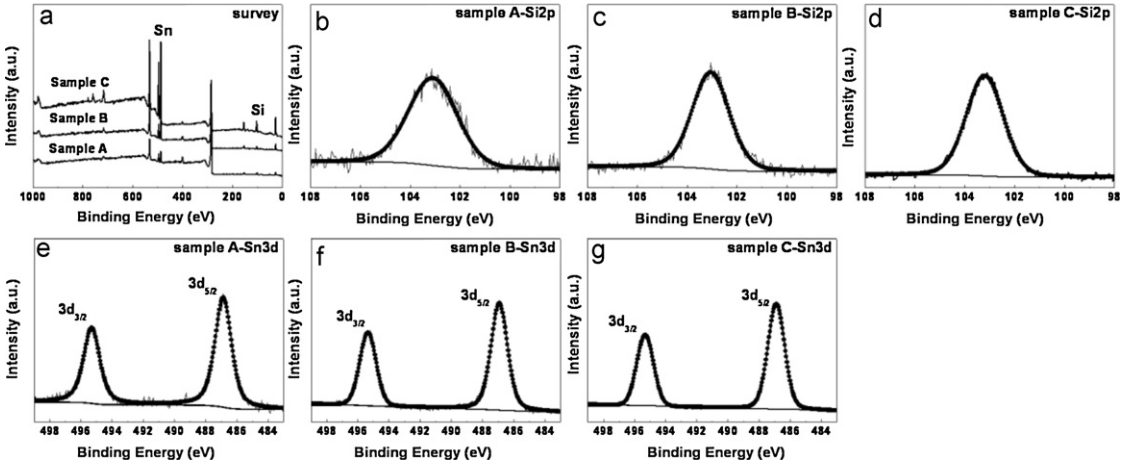

Fig. 3. XPS spectra of (a) the survey data, the Si 2*p* core level for ((b)–(d)) samples A, B, and C, and the Sn 3*d* core level for ((e)–(g)) samples A, B, and C.

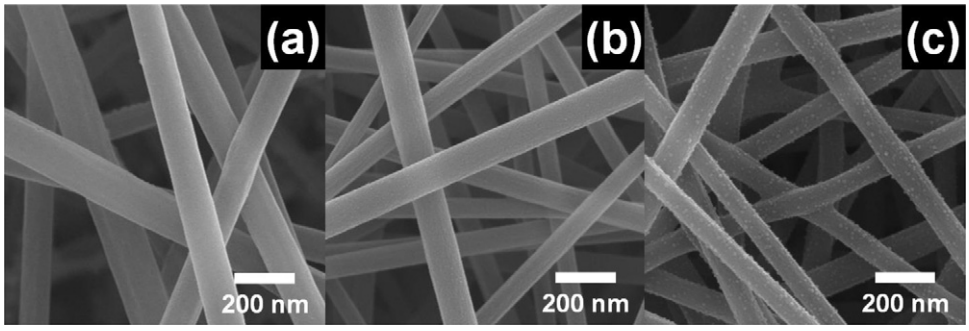

Fig. 4. FESEM images of ((a)–(c)) samples A, B, and C.

corresponding to elemental Sn in SnO_2 [11]. The XPS results show that the elemental Si in SiO_2 and the elemental Sn in SnO_2 are present as Si(IV) and Sn(IV) species.

Fig. 4 shows the FESEM images obtained from samples A, B, and C after they are calcined at 800 °C. This figure shows that the diameters of the CNF composites are in the range of ~104 to ~138 nm for sample A, ~73 to ~118 nm for sample B, and ~66 to ~110 nm for sample C. FESEM results confirm the successful formation of CNF composites including SnO_2 and SiO_2 nanoparticles. In addition, samples

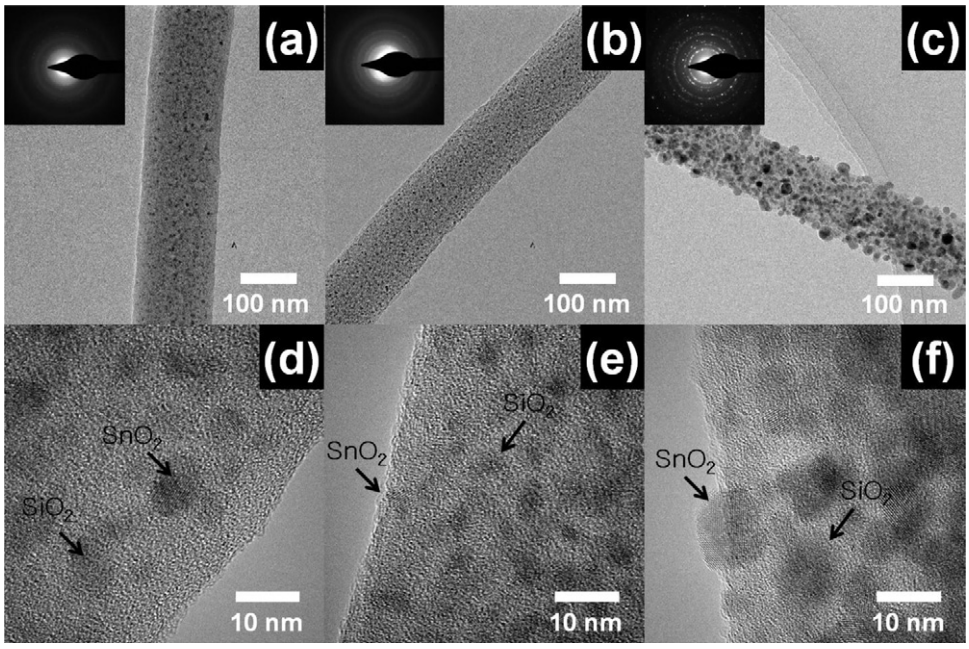

Fig. 5. TEM images and SAED patterns obtained from ((a)–(c)) samples A, B, and C and HRTEM images for ((d)–(f)) samples A, B, and C.

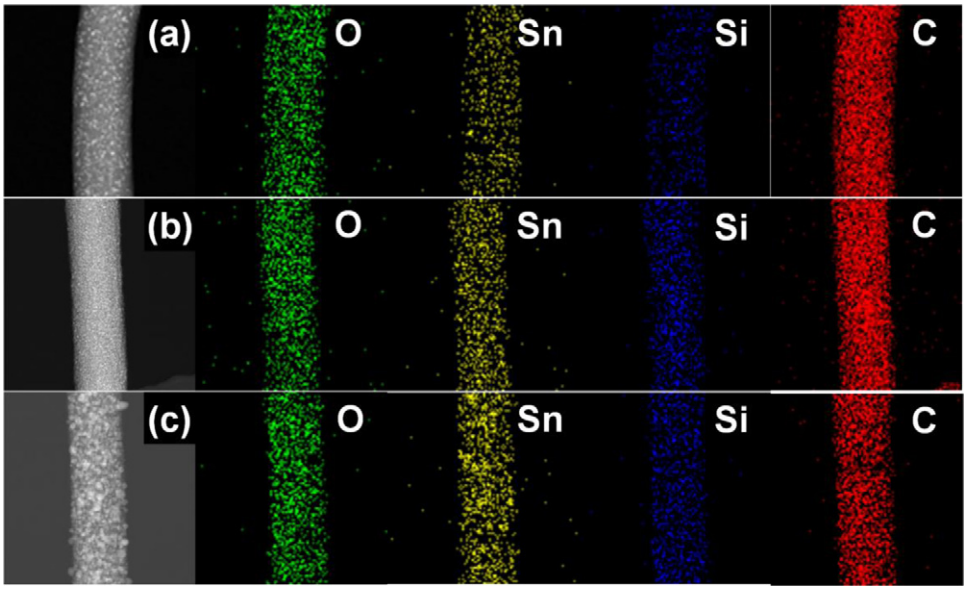

Fig. 6. TEM images and TEM-EDS mapping data obtained from ((a)–(c)) samples A, B, and C.

A and B (Fig. 4(a)–(b)) exhibit a smooth surface on the CNF composites; however, sample C exhibits a rough surface on the CNF composites, indicating that SnO_2 or SiO_2 nanoparticles are formed on the surface of the CNF composites as well as within the CNF composites.

To further investigate the morphology and structural properties, TEM examinations were carried out. Fig. 5 shows the TEM images and SAED patterns of samples A, B, and C after they are calcined at 800 °C. The diameters of the CNF composites are ∼130 nm for sample A, ∼110 nm for sample B, and ∼106 nm for sample C. In particular, SnO_2 and SiO_2 nanoparticles are well distributed in the CNF composites as shown in Fig. 5(a)–(c). The size of the SnO_2 and SiO_2 nanoparticles in the CNFs is in the range of ∼3–7 nm for sample A, ∼3–7 nm for sample B, and ∼5–14 nm for sample C, as shown in Fig. 5(d)–(f). Thus, the size and amount of SnO_2 and SiO_2 nanoparticles in the CNFs increase with the enhancing amount of Sn and Si precursors. TEM results, which are in good agreement with the XRD results, confirm that the SnO_2 nanoparticles have a crystalline structure relative to the long-range order of atoms and that the SiO_2 nanoparticles have an amorphous structure relative to the long-range disorder of atoms (see arrow in Fig. 5(d)–(f)). The SAED patterns (the insets in Fig. 5(a)–(c)) show a sharp ring around the (0 0 0) spot relative to the SnO_2 nanoparticles as well as a broad diffuse ring around the (0 0 0) spot relative to the SiO_2 nanoparticles.

To confirm a distributed composition of the SnO_2 and SiO_2 nanoparticles, TEM-EDS mapping examinations were carried out as shown in Fig. 6(a)–(c). The EDS mapping results indicate that Sn and Si atoms are uniformly distributed in the CNF, which implies that the SnO_2 and SiO_2 nanoparticles are well distributed in the CNF matrix. Thus, CNF composites consisting of crystalline SnO_2 and amorphous SiO_2 nanoparticles in the CNF have been successfully synthesized via co-electrospinning.

4. Conclusions

CNF composites consisting of SnO_2 and SiO_2 nanoparticles in the CNF were synthesized by co-electrospinning, and their structural characteristics and chemical compositions were shown by XRD, XPS, FESEM, TEM, and TEM-EDS mapping. The SnO_2 and SiO_2 nanoparticles were well distributed in the CNF matrix. The size and amount of the SnO_2 and SiO_2 nanoparticles in the CNF increased with the increasing amount of Sn and Si precursors. Therefore, a co-electrospinning technique can be regarded as one of the most powerful methods for fabricating CNF composites including three types of phases.

Acknowledgement

This research was supported by Basic Science Research Program through the National Research Foundation of Korea (NRF) funded by the Ministry of Education, Science and Technology (2011-0005561).

References

[1] H. Zhu, J. Wei, K. Wang, D. Wu, Applications of carbon materials in photovoltaic solar cells, Sol. Energy Mater. Sol. Cells 97 (2009) 1461–1470.
[2] E. Frackowiak, F. Beguin, Carbon materials for the electrochemical storage of energy in capacitors, Carbon 39 (2001) 937–950.
[3] S. Bal, Experimental study of mechanical and electrical properties of carbon nanofiber/epoxy composites, Mater. Des. 31 (2010) 2406–2413.
[4] M.H. Al-Saleh, U. Sundararaj, A review of vapor grown carbon nanofiber/polymer conductive composites, Carbon 47 (2009) 2–22.
[5] D. Li, Y. Wang, Y. Xia, Electrospinning of polymeric and ceramic nanofibers as uniaxially aligned arrays, Nano Lett. 3 (2003) 1167–1171.
[6] G.H. An, S.Y. Jeong, T.Y. Seong, H.J. Ahn, One-pot fabrication of hollow SiO_2 nanowires via an electrospinning technique, Mater. Lett. 65 (2011) 2377–2380.

[7] A. Mahapatra, B.G. Mishra, G. Hota, Synthesis of ultra-fine α-Al_2O_3 fibers via electrospinning method, Ceram. Int. 37 (2011) 2329–2333.
[8] H.R. Jung, S.J. Cho, K.N. Kim, W.J. Lee, Electrochemical properties of electrospun Cu_xO (x = 1,2)-embedded carbon nanofiber with EXAFS analysis, Electrochim. Acta 56 (2011) 6722–6731.
[9] L. Ji, X. Zhang, Manganese oxide nanoparticle-loaded porous carbon nanofibers as anode materials for high-performance lithium-ion batteries, Electrochem. Commun. 11 (2009) 795–798.
[10] S. Nagamine, S. Ishimaru, K. Taki, M. Ohshima, Fabrication of carbon-core/TiO_2-sheath nanofibers by carbonization of poly(vinyl alcohol)/TiO_2 composite nanofibers prepared via electrospinning and an interfacial sol–gel reaction, Mater. Lett. 65 (2011) 3027–3029.
[11] J.F. Moulder, W.F. Stickle, P.E. Sobol, K.D. Bomben, Handbook of X-ray Photoelectron Spectroscopy, Physical Electronics, Inc., Physical Electronics, Eden Pairie, 1995, pp. 57–127.